

IDENTIFICATION OF LOCALIZED ROUGHNESS FEATURES AND THEIR IMPACT ON VEHICLE DURABILITY

Graduate of Polytechnic School of Tunisia, 2004. Completed a master degree in 2005 in applied math to computer science and a M.S. degree in 2008 in civil engineering. Currently a research assistant and Ph.D. candidate in the civil and environmental engineering department at Michigan State University.
Email: zaabarim@egr.msu.edu



Imen ZAABAR
Michigan State University
USA



Karim CHATTI
Michigan State University
USA

Obtained B.S. and M.S. from Michigan State University, USA, in 1985 and 1987 and a Ph.D. degree in Pavement Engineering from the University of California-Berkeley in 1992. Joined the civil and environmental engineering department at MSU in 1993 where he is currently a Professor.
Email: chatti@egr.msu.edu

Abstract

Vehicle manufacturers place a major focus on improving the design of vehicle components to respond better to changes in road surface profiles. Despite this, changes in the surface profile still directly affect the user costs including repair and maintenance costs and damage to goods. For example, the Federal Highway Administration (FHWA) reported that poor road conditions added an estimated 768 billion dollars to transport costs annually. Roughness features detection methods detect, locate and identify the level of surface irregularities; however, they do not in themselves provide guidance on acceptable roughness levels to limit user costs. The objective of this study is to provide guidance on acceptable roughness levels to limit user costs using vehicle-road interaction models. Accordingly, we propose using a mechanistic-empirical approach to conduct fatigue damage analysis using numerical modeling of vehicle response.

Keywords: Repair and maintenance costs, Roughness features, Guidance.

1. Introduction

All road surfaces have some level of roughness even when they are new, and they become increasingly rougher with age depending on pavement type, traffic volume, environment etc. This process is mainly driven by the interaction between vehicles and pavements. An increase in pavement roughness leads to higher dynamic loads. This amplification in the load magnitude can lead to a tangible acceleration in pavement distress. The pavement distresses lead to surface irregularities which translate into a transient event in the raw profile affecting the ride quality of a road. The surface profile of the road transmits the vibrations through the tires and suspension system to the body of the vehicle and then to the driver, passengers and cargo. Vehicle manufacturers place a major focus on constantly improving the design of these different vehicle components to respond better to changes in road surface profiles. Despite this, changes in the road surface profile still directly affect the user costs including repair and maintenance costs. For example, the Federal Highway Administration (FHWA)

reported that poor road conditions added an estimated 768 billion dollars to transport costs annually.

State Highway Agencies extract pavement surface distresses (type, extent, and severity) from video images of the pavement surface biannually. The collection of distress data from video imaging of the pavement surface can provide the location and type of many distresses. However, they do not retain the actual contents of pavement surface roughness. Such detailed roughness information may be useful for maintenance operations. Failure to include specific roughness features in Pavement Management Systems (PMS) will underestimate user costs including repair and maintenance and damage to goods. Therefore, a significant improvement to the field would be the implementation of tools to extract localized roughness features associated with certain pavement distresses, through the use of the raw profile data. The developed tools detect, locate and identify the level of surface irregularities; however, they do not in themselves provide guidance on acceptable roughness levels to limit user costs. The objective of this paper is to develop a methodology to determine such roughness threshold. If this threshold value exists, it could be a useful preventive maintenance (PM) tool, whereby a PM action, such as smoothing the pavement surface, is taken to reduce user costs.

2. Background

2.1 Pavement roughness features

Roughness features are important factors in pavement design and management. Their evaluation is an important part of the pavement management system by which a most effective strategy for maintenance and rehabilitation can be developed. Our concern in this paper is the detection of faults, breaks and curling in concrete pavements and potholes in asphalt pavements. The definitions of each of these roughness features are summarized below (Huang, 2003).

Faulting

Faulting is the difference in elevation across a joint or crack. It is determined by measuring the difference in elevation between the approach slab and the adjacent slab. In the current practice of road surface profile measurement in the US, the reporting interval for elevation is 0.025 to 0.075 m (1 to 3 inches). Based on previous study by Chatti et al (2008), for a sampling interval of 0.019 m and a reporting interval of 0.075 m, the correct height of a fault is detectable when it is calculated as the difference in elevation between points that are 0.15 m apart. Accordingly, the width of a fault was taken as this value.

Breaks

Break is a broken portion of the pavement section that starts with a negative fault and ends with a positive fault. The distance between the two opposite faults should not exceed 0.9 m (3ft), see Huang (2003).

Curling

Curling is the distortion of a slab into a curved shape by upward or downward bending of the edges. This distortion can lift the edges of the slab from the base leaving an unsupported edge or corner which can crack when heavy loads are applied. Sometimes, curling is evident at any early age. In other cases, slabs may curl over an extended period of time.

Potholes

A pothole is when a portion of the road material has broken away, leaving a hole. Most potholes are formed due to fatigue of the pavement surface. As fatigue cracks develop they typically interlock in a pattern known as "alligator cracking". Then, the pavements between fatigue cracks become loose by continued wheel loads forming a pothole. The width of a pothole was taken as 0.9 m (3ft), similarly to breaks.

2.2 Rigid Pavement Types

Jointed plain concrete pavement (JPCP)

This is the most common type of rigid pavement. JPCP controls cracks by dividing the pavement into individual slabs separated by contraction joints. Slabs are typically between 3.7 m (12 ft.) and 6.1 m (20 ft.) long.

Jointed reinforced concrete pavement (JRCP)

JRCP slabs are much longer (as long as 15 m (50 ft.)) than JPCP slabs; so JRCP uses reinforcing steel within each slab to control cracking. This pavement type is no longer constructed in the U.S. due to some long-term performance problems.

3. Research Approach

The mechanistic-empirical approach, that was proposed to quantify the effect of roughness features characteristics on vehicle suspension, consists of the following steps:

1. Artificial generation of road surface profile;
2. Artificial generation of roughness features (bumps, depressions and curling);
3. Estimation of the response of the vehicle to these transient events;
4. Computing of the induced damage to the vehicle suspension;
5. Repeat step 2 through 4 for different heights and frequencies of roughness features.

3.1 Artificial Generation of Profiles and Roughness Features

Artificial generation of road surface profiles

The pavement surface roughness profiles were generated from the equation suggested by (Robson, 1979):

$$S_u(k) = c|k|^{-n} \quad (1)$$

where:

$$\begin{aligned} S_u(k) &= \text{displacement spectral density,} \\ &\quad \text{m}^3/\text{cycle} \\ n &= 2.5 \\ k &= \text{wavenumber} \end{aligned}$$

The constant c in Equation 1 was found to be correlated with the IRI (Hardy and Cebon, 1995) and could be estimated using Equation (2):

$$c \approx 1.69 \times 10^{-8} (\text{IRI})^2 \left(m^{1/2} \text{cycle}^{3/2} \right) \square \square \quad (2)$$

To generate a random road surface profile, a set of random phase angles uniformly distributed between 0 and 2π is applied to the desired spectral density. Then, the inverse discrete Fourier transform was applied to the spectral coefficients (Cebon, 1997).

Artificial generation of roughness features

The focus of this paper is to provide guidance on acceptable roughness levels to limit user costs. The identified roughness features that were proven to affect vehicle suspensions are: faulting, breaks and curling in concrete pavements and potholes in asphalt pavements. To investigate their effect, these roughness features were artificially generated and superimposed on to the generated road surface profile. The resulting road profile over 1.6 km is:

$$u(x) = u_r(x) + u_f(x) \quad (3)$$

where

$u_r(x)$ = road surface profile

$u_f(x)$ = roughness features

$$= \begin{cases} u_{jf}(x) & \frac{i * 1600}{N} \leq x \leq \frac{i * 1600}{N} + h; \quad i = 1 : N; \quad x + h < 1600m \\ 0 & \text{Otherwise} \end{cases}$$

N = number of roughness features per 1.6 km

H = width of the roughness features

$U_{jf}(x)$ = roughness feature (Figure 1)

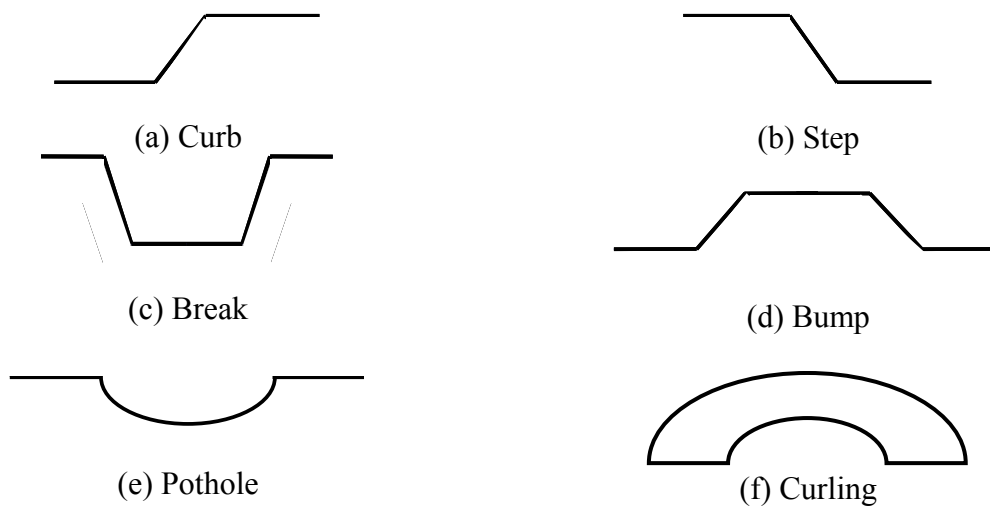


Figure 1 – Schematic description of roughness features

3.2 Methods to Identify Roughness Features

In the study conducted by Chatti et al. (2008), five methods were considered for identifying roughness features from a profile: (1) Discrete Elevation Difference method (DED); (2) Discrete Slope method (DS); (3) Discrete Curvature method (DC); (4) Wavelet analysis method; and (5) Time-frequency analysis. Many time-frequency analysis approaches were

performed including Wigner-Ville Distribution (WVD), Pseudo WVD (PWVD), and Smoothed Pseudo WVD (SPWVD), Short Time Fourier Transform (STFT) using different cutoff windows (Hamming, Hanning, Gabor distribution, etc). Although, the joint time frequency analysis method is powerful for electrical and mechanical signals, it was found not to be effective for the analysis of pavement profiles (except for wavelet transforms). Specifically, the following issues were noted:

1. The non-linearity of the Wigner distribution causes many interference phenomena, which make it less attractive for detection purposes.
2. The STFT has also its disadvantages, such as the limit in its time-frequency resolution capability, which is due to the uncertainty principle. Low frequencies can be hardly depicted with short windows, whereas short pulses can only be poorly localized in time with long windows. These limitations in the resolution were some of the reasons for the invention of Wavelet theory.
3. Although the Cohen's class distribution function has higher clarity than STFT and Wigner distribution, it still suffers from an inherent cross-term (interference) contamination when analyzing multi-component signals.

It was found that the wavelet analysis, the DED and DS methods give better results. These methods were able to extract the magnitude and location of roughness features with the same order of error. However, the DED and DS method were selected in this study for their simplicity. The DED method was selected for detecting faults, breaks and potholes. The DS method was selected for curling detection. The average error and the standard deviation of these methods were 0.1% and 1% respectively. The localization was also highly accurate (average error in distance is within 1 m or 0.5%).

3.3 Dynamic Vehicle Simulation

A number of vehicle models have been developed to describe the dynamic behavior of vehicles ranging from quarter to full vehicles as reported by (Cebon, 1999). It has been suggested, however, that in most cases, the vertical mode remains the dominant component of vibration induced by irregular pavement surfaces. It is well understood that quarter-car models cannot be expected to predict loads on a physical vehicle exactly, but it will highlight the most important road characteristics as far as fatigue damage accumulation is concerned; it might be viewed as a "fatigue-load filter". Therefore, a quarter-car model was used in this study. The quarter-car model is represented by a second-order, two-degree-of-freedom, linear differential equation system [Equations (4) and (5)], whereby the vehicle response is computed for the vertical orientation with the pavement irregularities as the excitation function.

$$m_u \ddot{x}_u - c_s (\dot{x}_s - \dot{x}_u) - k_s (x_s - x_u) + k_t (x_u - u) = 0 \quad (4)$$

$$m_s \ddot{x}_s + c_s (\dot{x}_s - \dot{x}_u) + k_s (x_s - x_u) = 0 \quad (5)$$

where:

- u(t)** = road profile elevation
- x_u** = elevation of unsprung mass (axle)
- x_s** = elevation of sprung mass (body)
- k_t** = tire spring constant

- k_s = suspension spring constant
- c_s = shock absorber constant
- m_u = unsprung mass (axle)
- m_s = sprung mass.

‘Quarter car’ parameters for a full truck with typical air and steel suspensions from (Cole and Cebon, 1997) are given in Figure 2.

		Model parameters	
	Unit	Steel	Air
m_s	Kg	4500	4500
m_u	Kg	500	500
k_s	MN/m	1	0.4
k_t	MN/m	2	2
c_s	KNs/m	20	20

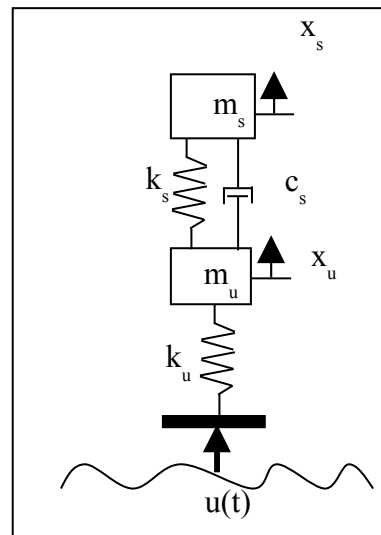


Figure 2 – Schematic of Two Degrees of Freedom Quarter-Car Vehicle Model

A simple generic linear numerical quarter-vehicle model was developed to compute the vertical vibration level of typical vehicle types from different pavement profiles at constant speeds. This numerical model developed with the Matlab/Simulink® programming environment effectively computes the solution to the two degrees of freedom system. The inputs to the model are the longitudinal pavement profile and the velocity of the vehicle.

3.4 Vehicle Fatigue Damage Analysis

A common laboratory experiment to predict fatigue damage is to subject test specimens to a sinusoidal load with amplitude U , and count the number of cycles N to breakdown. Commonly, the simple parametric model $N(U) = C^{-1}U^{-\beta}$ (Basquin’s relation) is fitted to experimental data. Usually, for vehicle components, the fatigue exponent β takes values between 3 and 8 (Bogsjö, 2006). A typical β value for steel suspensions is 6.3 upon a “half-life” rule (Fuchs and Stephens, 1980). The “half-life” rule states that the half life of a steel component will be approximated at a 10 to 12% increase in cyclic load amplitude.

Loads caused by road roughness fluctuate randomly. To assess the fatigue damage, it is necessary to extract cycles from the load sequence.

The load sequence on the sprung mass of the vehicle model is rainflowcounted, to extract the load cycles U_i . The rainflow counting method was introduced by (Endo, 1968). A simplified equivalent definition was given by (Rychlik, 1987). This definition (stated below) can be used to extract cycles straight-forwardly, see also Figure 3.

Definition (Rainflow cycle). Each local maximum in the load sequence is paired with one particular local minimum, determined as follows (Figure 3): From the i^{th} local maximum (value M_i) one determines the lowest values in forward and backward directions between M_i and the nearest points at which the load exceeds M_i . The minima m_i^- and m_i^+ on each side are identified.

The larger (less negative) of those two values, denoted by m_i^{RFC} , is the rainflow minimum paired with M_i , i.e. m_i^{RFC} is the least drop before reaching the value M_i again on either side. Thus the i^{th} rainflow pair is (M_i, m_i^{RFC}) and the rainflow amplitude is $U_i = M_i - m_i^{RFC}$

Palmgren-Miner's linear accumulation hypothesis is used to estimate fatigue damage. Thus, the damage caused by the j^{th} cycle equals $1/N(U_j)$, where $U_j = M_j - m_j^{RFC}$. The total fatigue damage caused by the rainflow-counted load sequence is:

$$D = C \sum_i U_i^\beta \quad (6)$$

Computations of fatigue damage from a given load sequence is performed using MATLAB.

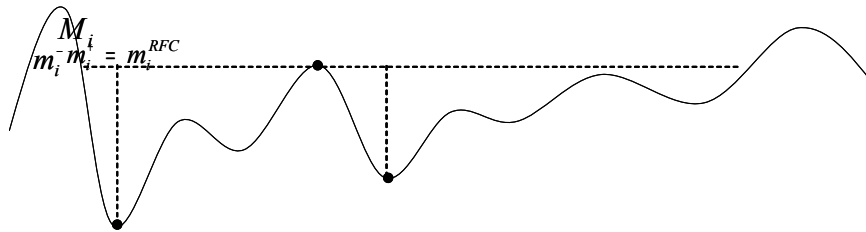


Figure 3 – Definition of the rainflow cycle as given by (Rychlik, 1987)

4. Guidance on Acceptable Roughness Levels

4.1 Introduction

To illustrate the various features of the method described above, the case study of US conditions has been examined. All road surface profiles were artificially generated at every 0.07 m. Road surface profiles were filtered out using a moving average filter with a baselength of 0.3 m representing the tire enveloping. Then, the ‘quarter car’ vehicle models traveling at a constant speed of 110km/h were applied to a 1.6 km of road surface profiles. The parameters used in the ‘quarter car’ model are given in Figure 1 above.

Based on personal communications with auto repair specialists (2008), truck owners tend to replace their suspensions at about 400000 km. This value was also reported as the lifetime warranty for suspensions given by truck manufacturers in the US. Consequently, in this study, the average life of truck suspensions for typical driving conditions was assumed to be about 400000 km.

Moreover, truck suspensions are not replaced when they actually fail but when certain signs of wear become evident and, consequently, compromise the safety and comfort of drivers. The amount of service life at which owners are urged to replace their suspensions was estimated using the following procedure:

1. Estimate the roughness (IRI) distribution of US roads (Figure 4), with 1 m/km corresponding to a smooth road and 6 m/km to a very rough road;
2. Generate road surface profiles for different IRI values;
3. Calculate the accumulated damage (D_{IRI}^j) induced by road roughness for a length of 1.6 km and assuming a value of 6.3 for β in Equation 6;
4. Estimate the number of kilometers per IRI (L_{IRI}^j) value using the distribution obtained in step 1 and assuming that the road network is 400000 km.
5. Compute the total accumulated damage using Equation 7:

$$D_{replace} = \sum_{i=1}^N \left(D_{IRI_i}^j \times L_{IRI_i}^j \right) \quad (7)$$

Using the above procedure, the value for $D_{replace}$ is about 62.2 %.

Based on personal communication with PACCAR Inc. (2007) and SoMat (2009), many automotive companies design their vehicles for the 80th-95th percentile road roughness. According to Figure 4, 3.2 m/km is the 87th percentile of the roughness distribution in the US. From Figure 5, when a truck is driven over a 400000 km of road with IRI = 3.2 m/km, the accumulated suspension damage will be about 66%, which is very close to 62.2%. Therefore, we proved using two different methods that a value of 6.3 for β is reasonable. Accordingly, a typical value for β is taken as this value.

The additional cost induced by roughness features when the accumulated damage reaches $D_{replace}$ was assumed to be equal to the price of a new suspension and the labor hours for replacement (i.e., \$3000 and \$1800 for air and steel suspensions, respectively, according to auto repair specialists (2008)).

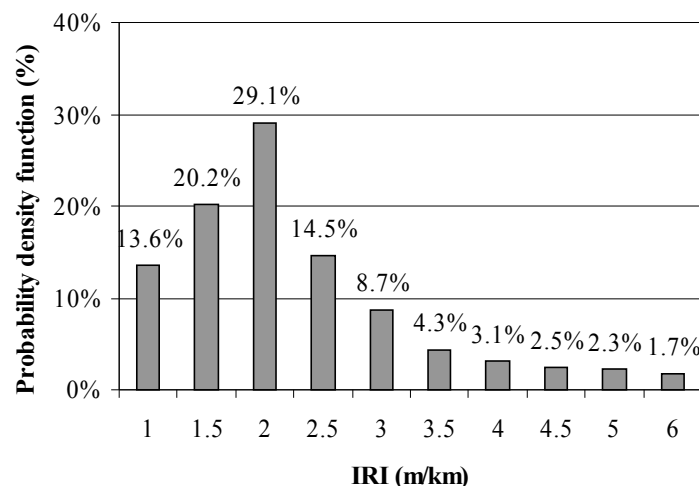


Figure 4 – Road surface roughness distribution in the United States

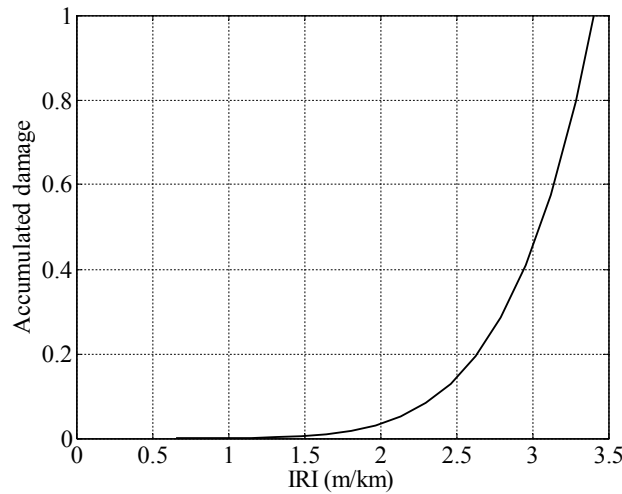


Figure 5 – Effect of road surface roughness on vehicle suspension damage

4.2 Results

The first case study examines the effect of different combinations of faulting levels and frequencies per 1.6 km on both air and steel suspensions. The faulting was modeled as a rising step function of variable amplitude and a length of 0.15 m. The vehicle speed was the same for all the runs. Figures 6 and 7 show the repair and maintenance costs for different levels and frequencies of faulting for JRCP and JPCP pavements, respectively. The costs were expressed as dollars per 1000 km. As expected, the effect of faulting on air suspensions is lower than on steel suspensions because air suspensions provide more vibration isolation. However, the additional repair and maintenance costs for air and steel suspensions are similar because replacing air springs is much more expensive than replacing a steel suspension.

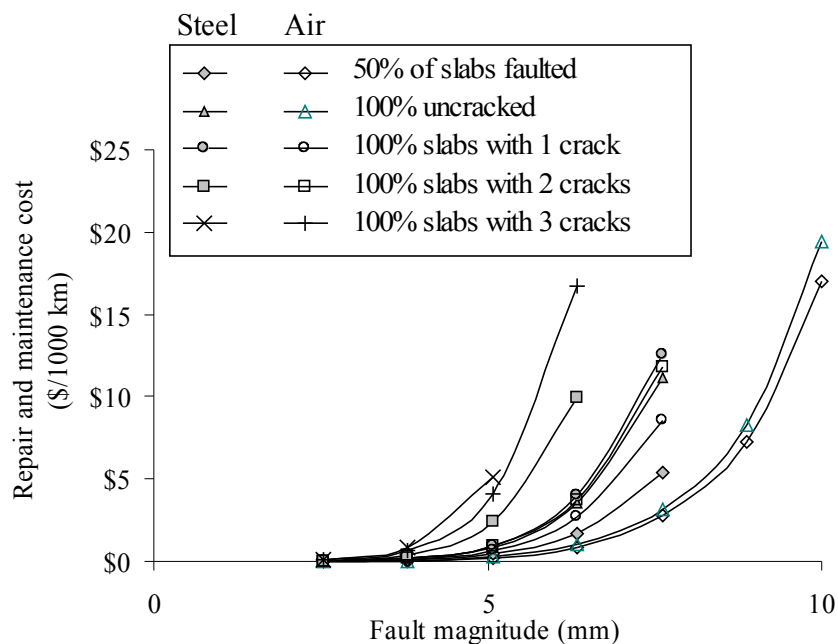


Figure 6 – Repair and maintenance costs induced by different levels of faulting - JRCP

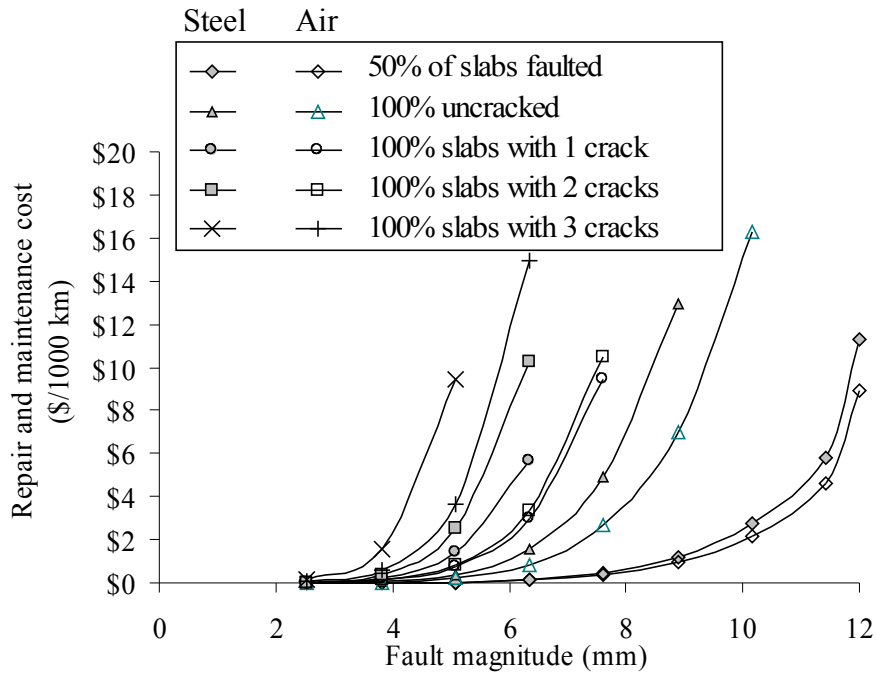


Figure 7 – Repair and maintenance costs induced by different levels of faulting - JPCP

The second case study examines the effect of different combinations of breaks/potholes levels and frequencies per 1.6 km on both air and steel suspensions. The breaks were modeled as a step function of variable amplitude and a length of 0.9 m. Figure 8 shows the repair and maintenance costs for different severity levels of breaks. The effect of breaks on air suspensions is much lower than on steel suspensions. Even though replacing air springs is much more expensive than replacing steel suspension, the additional repair and maintenance costs for air suspensions induced by multiple passes over breaks are less than those for steel suspensions.

The third case study examines the effect of different combinations of curling magnitude and frequencies for 1.6 km of Jointed Reinforced Concrete Pavements (JRCP) on both air and steel suspensions. Curling is modeled as a half-sine function of variable amplitude and length. The slab width for JRCP is 12.5 m (41 ft). These conditions were analyzed for (1) uncracked slabs, (2) slabs with one mid-panel crack, and (3) slabs with 2 mid-panel cracks. Figure 9 shows the additional repair and maintenance costs caused by different severity levels of curling. The additional repair and maintenance costs for air suspensions induced by multiple passes over curled slabs are much less than those for steel suspensions. Since the road isolation ability of air ride suspensions is higher than leaf spring suspensions, they will absorb more energy induced by the vertically accelerated wheel, allowing the frame and body to ride undisturbed while the wheels follow the bumps in the road.

The fourth case study examines the effect of different combinations of curling magnitude and frequencies for 1.6 km of Jointed Plain Concrete Pavements (JPCP) on both air and steel suspensions. The slab width for JPCP is 4.5 m (15 ft). It was noted that the additional repair and maintenance costs caused by curling in JPCP pavements (Figure 10) is lower than those

induced by curling in JRCP pavements. We believe that the slab length being smaller for JPCP induced higher dynamic loads. This increase led to additional damage.

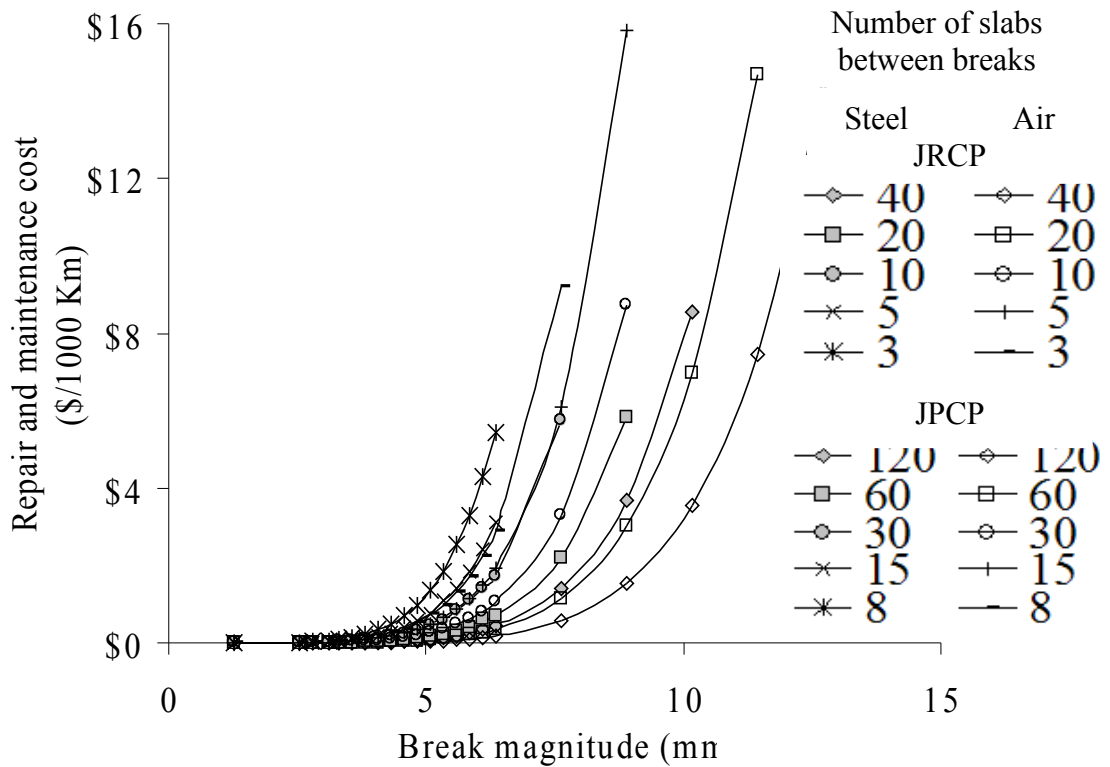


Figure 8 – Repair and maintenance costs induced by different levels of breaks

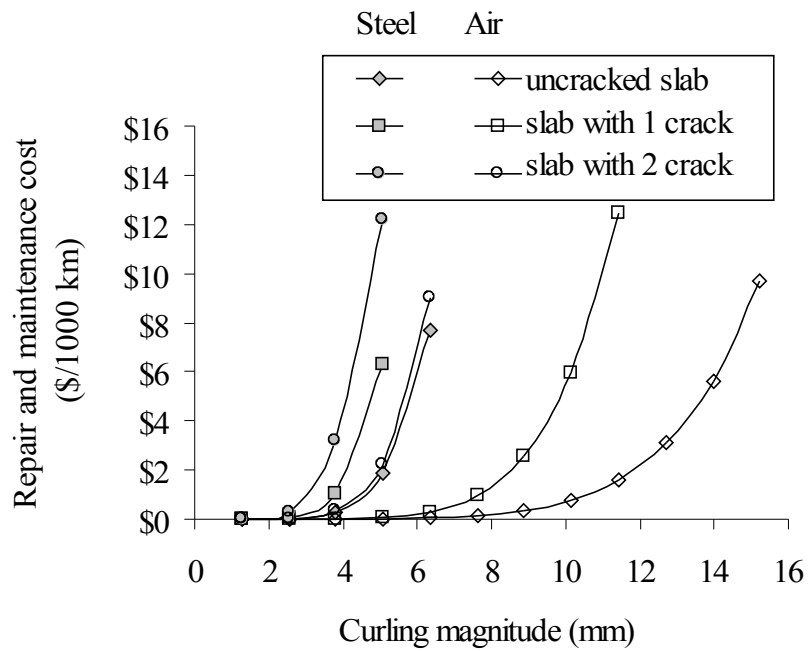


Figure 9 – Repair and maintenance costs induced by different levels of curling - JRCP

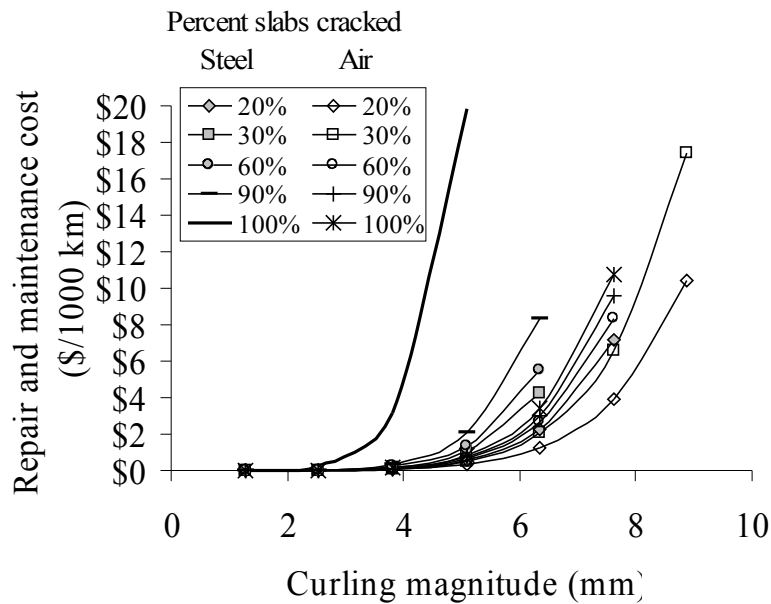


Figure 10– Repair and maintenance costs induced by different levels of curling – JPCP

5. Conclusions and Recommendations

In this paper, we proposed a novel approach to estimate the additional repair and maintenance costs induced by roughness features. We proposed using a mechanistic-empirical approach to conduct vehicle suspension fatigue damage analysis using numerical modeling of vehicle vibration response. In this study, we used the quarter-car model which is represented by a second-order, two-degree-of-freedom system since, in most cases, the vertical mode remains the dominant component of vibration induced by irregular pavement surfaces. The results reported in this paper could help in better estimating vehicle operating costs at the project level, which are essential to sound planning and management of highway investments, especially under increasing infrastructure demands and limited budget resources.

6. References

- Bogsjö, K. (2006), “Development of analysis tools and stochastic models of road profiles regarding their influence on heavy vehicle fatigue”, *Vehicle System Dynamics*, 44, Supplement, 780-790.
- Chatti, K., Zaabar, I., and Lee, H.S. (2008), “Development of a simple diagnosis tool for detecting localized roughness features” in *Proceeding of the 9th International Conference on Concrete Pavements*, 673-689.
- Cebon, D. (1999), *Handbook of Vehicle-Road Interaction*, Swets & Zeitlinger, Lisse, Netherlands.

- Cole D.J. and Cebon D. (1997), “Effects of ‘road friendly’ suspensions on long-term flexible pavement performance”, Proceedings of the Institution of Mechanical Engineers, Part C: Journal of Mechanical Engineering Science, 211(6), 411-424.
- Fuchs, H.O. and Stephens, R.I. (1980), Metal Fatigue in Engineering, John Wiley & Sons, 155-156.
- Hardy M.S.A. and Cebon D. (1995), “An investigation of anti-lock braking strategies for heavy goods vehicles”, Journal of Automobile Engineering, Institute of Mechanical Engineers, 209(D4), 263-271.
- Huang, Y. H. (2003), Pavement Analysis and Design, Prentice Hall.
- Matsuiski, M. and Endo, T. (1969), “Fatigue of metals subjected to varying stress”, Japan Society of Mechanical Engineering.
- Rychlik, I (1987), “A new definition of the rainflow cycle counting method”, International journal of fatigue, 9, 119-121.
- Consumer Reports and personal communication with auto repair specialists (2008), www.repairpal.com
- <http://www.paccar.com/> (2007)
- Janas, J. (2002), "Relating road roughness to vehicle component fatigue", EE-Evaluation Engineering, SoMat.